ADVANCED OPTICAL MATERIALS
www.advopticalmat.de

Optical Outcoupling Efficiency of Organic Light-Emitting Diodes with a Broad Recombination Profile

Yungui Li, Naresh B. Kotadiya, Bas van der Zee, Paul W. M. Blom, and Gert-Jan A. H. Wetzelaer**

Although a broadened recombination zone is beneficial for the lifetime of organic light-emitting diodes (OLEDs), its effect on the optical outcoupling efficiency is unknown. Here, a numerical model to simulate the fraction of photons coupled to air for devices with a broad recombination zone is presented. It is demonstrated that the total outcoupling can be calculated as the integral of the outcoupling efficiency over different positions of emitting dipoles, weighted by the sum-normalized recombination profile, as obtained from electrical modeling. Using single-layer OLEDs based on the thermally delayed activated fluorescence emitter 9,10-bis(4-(9H-carbazol-9-yl)-2,6-dimethylphenyl)-9,10-diboraanthracene (CzDBA) as a model system, it is demonstrated that an outcoupling efficiency to the air mode as high as ≈26% can be obtained. These simulations are validated with experiments on CzDBA OLEDs of different thickness. The results show that single-layer devices with a broadened emission zone can achieve similar outcoupling efficiency to multilayer OLEDs with an optimized confined emission zone, establishing a route to efficient, stable, and simplified OLEDs.

1. Introduction

Impressive progress has been made for organic light-emitting diodes (OLEDs) ever since the first report by Tang and VanSlyke in 1987.[1] The development of organic doping,[2] phosphorescent emitters,[3] and light outcoupling strategies[4] has significantly improved the device efficiency. However, the high cost of phosphorescent emitters as well as the shorter lifetime of blue OLEDs compared to its green and red counterparts poses a great challenge to both scientific and industrial communities. The invention of purely organic emitters that can transfer non-radiative triplet excitons to emissive singlet excitons aided by thermal energy from the ambient environment, known as thermally activated delayed fluorescence (TADF), opens an avenue to develop cost-effective OLEDs.[5] Devices based on TADF emitters with comparable or even higher efficiency compared to phosphorescent emitters have been reported, demonstrating their promising application potential.[6] One of the most important research targets now is to enhance the device lifetime.[7–9]

Very recently, we demonstrated efficient and long-lived OLEDs based on the TADF emitter 9,10-bis(4-(9H-carbazol-9-yl)-2,6-dimethylphenyl)-9,10-diboraanthracene (CzDBA) by using an unconventional single-layer device configuration. In this simplified device architecture, the widely used blocking and transport layers, as well as co-evaporated guest-host layers are not needed.[10–12] With a neat film of CzDBA (75 nm), sandwiched between two Ohmic contacts employing thin interlayers,[13,14] a maximum external quantum efficiency (η_{EQE}) of ≈19% can be obtained. Due to the Ohmic contacts, absence of heterojunctions and near-trap-free charge transport, very low operating voltages are achieved, resulting in high power efficiencies. Additionally, a lifetime of 1880 h was measured during which the luminance decreased to 50% of its initial value (LT_{50}), for an initial luminance at 1000 cd m^{-2}. Remarkably, this lifetime is almost a factor of 20 longer compared to the LT_{50} lifetime (97 h) reported for conventional multi-layer devices, using the same emitter. In this multi-layer structure, the generated excitons are confined to a thin emissive layer of 30 nm.[15] For the single-layer device, recombination events exist within the entire active layer.[10] It has been previously demonstrated that the broadening of the recombination zone reduces the exciton concentration under operation.[16,17] For single-layer polymer based LEDs it has been shown that the rise of operation voltage and decrease of light-output under constant electrical current is the result of the formation of hole traps due to exciton–polaron interactions.[18] A spatial broadening of the recombination profile simultaneously lowers the exciton and polaron concentration and is therefore beneficial for the lifetime. Furthermore, a reduced exciton concentration also lowers the possibility of mutual exciton annihilation.[19,20]

Although the lifetime of TADF OLEDs with a wide recombination zone is superior to those with a confined emission layer, the question arises what the effect of the spatially distributed emission zone on the light-outcoupling efficiency η_{out} is. In a

Dr. Y. Li, Dr. N. B. Kotaidya, B. van der Zee, Prof. P. W. M. Blom, Dr. G.-J. A. H. Wetzelaer
Max Planck Institute for Polymer Research
Ackermannweg 10, Mainz 55128, Germany
E-mail: yungui.li@mpip-mainz.mpg.de; wetzelaer@mpip-mainz.mpg.de
The ORCID identification number(s) for the author(s) of this article can be found under https://doi.org/10.1002/adom.202001812.

DOI: 10.1002/adom.202001812

multi-layer OLED, the position of the confined recombination zone can be shifted by tuning the thickness of the transport layers to optimize the optical outcoupling.[21,22] It is still unclear whether similar outcoupling efficiencies can be obtained in single-layer OLEDs with an extended recombination zone. Therefore, understanding of the optical behavior of OLEDs with a broad recombination profile is a prerequisite for the further development of devices that combine high efficiency and long lifetime in a simplified architecture. In this work, we present simulations of the fraction of photons evanescent to air and/or substrate modes in OLEDs with a broad recombination zone. We demonstrate that the outcoupling efficiency can be calculated as the integral of the local outcoupling efficiency of dipoles with emission from different positions within the broad recombination zone, weighted by a function of the sum-normalized recombination profile. Combining the optical model with electrical numerical drift-diffusion simulations that calculate the recombination profile, the fraction of generated photons evanescent to air mode η_A and the sum of substrate and air mode η_{SA} can be simulated. Using CzDBA single-layer OLEDs as a model system, it is demonstrated that an outcoupling efficiency to air up to 26.2% can be obtained, only marginally lower than the 28.0% obtained for a CzDBA OLED with an optimized position of the localized emitting plane. Combined with the experimental η_{EQE}, the estimated electrical efficiency reaches values as high as 92%. Overall, the combined optical and electrical simulations demonstrate that broadening of the emission zone, enhancing device stability, does not go at the expense of loss in performance due to optical effects. This finding paves the way for further developments of efficient and stable OLEDs with different emission spectra based on a highly simplified device structure.

2. Results and Discussion

2.1. Derivation of the Outcoupling Efficiency for OLEDs with a Broad Recombination Profile

As derived previously by Furno et al.,[23] in the steady state, without considering the exciton diffusion, non-radiative recombination, electrode quenching, and/or exciton annihilation processes, the total exciton concentration per unit volume per unit time can be written as:

$$\hat{n}_e = \int_z \xi G(z)\,dz \tag{1}$$

where the pre-factor ξ accounts for the fraction of generated exciton species (e.g., singlets and triplets) due to spin statistics upon electrical excitation, and G the exciton generation rate among different positions z.

For multi-layer devices, the exciton-generation zone $G(z)$ is usually treated as a delta function, that is, an ultrathin plane in the OLED. Due to this assumption the outcoupling efficiency can be estimated by only considering the optical properties of the OLED stack. By contrast, we here consider the case of devices with a spatially distributed recombination profile, in which the emission zone cannot be described by a delta function. As shown schematically in **Figure 1**a, the amount of outcoupled light is highly dependent on the position of emitters within the device. In an OLED with a broad emission zone, the actual recombination profile should be known to calculate the optical outcoupling efficiency. Such a recombination profile is governed by the electrical and recombination processes in the organic semiconductor and is obtained from a combination of charge transport studies and numerical drift-diffusion modelling. Therefore, to model the outcoupling of OLEDs with a broad emission zone we have developed an integrated optical and electrical OLED device model. In case that the shape of the recombination profile $g(z)$ is known for devices with a broad recombination zone, it is possible to obtain $G(z)$ as:

$$G(z) = \hat{A} \cdot g(z) \tag{2}$$

where $\hat{A}$ is the total exciton concentration generated per unit time integrated over the complete recombination profile. In such a scenario, the recombination profile $g(z)$ should be normalized to the integral over the total emissive layer, as to obtain:

$$\int_z g(z)\,dz = 1 \tag{3}$$

In such a case, the final form of η_{EQE} for OLEDs with a broad recombination zone can be written as:

$$\eta_{EQE} = \frac{e\xi}{J} \cdot \eta_{int}^{*} \cdot \hat{A} \int_z g(z)\eta_{out}(z)\,dz \tag{4}$$

where e is the elementary charge and η_{int}^{*} is the internal quantum efficiency for the emitter in the cavity. According to Equation (4), mathematically, the outcoupling efficiency η_{out} for OLEDs with a broad recombination zone can be treated as a numerical integration over $\eta_{out}(z)$ at different recombination positions, the weighting function being the sum-normalized recombination profile $g(z)$. Thus:

$$\eta_{out} = \int_z g(z)\eta_{out}(z)\,dz \tag{5}$$

For multi-layer OLEDs, where excitons are confined to a thin (≈10 nm) emissive layer, the sum-normalized recombination profile $g(z)$ is then reduced to a delta-function. However, when the emissive layer is broadened, this approximation is no longer valid.[23–25] In that case, according to Equation (5), it is then possible to simulate the fraction of photons that escape to the air mode η_A and the sum of the substrate and air mode η_{SA} by integrating over different recombination positions weighted by the sum-normalized recombination profile, as shown in Figure 1b.

2.2. Position Dependence of the Outcoupling Efficiency

As shown in Figure 1a, the outcoupling of photons from spontaneous radiation of excitons that can escape to the air mode is dependent on the dipole position within the device cavity.[22] The fraction of photons coupled to the air mode, substrate mode, waveguide mode, and surface plasmon polariton (SPP)

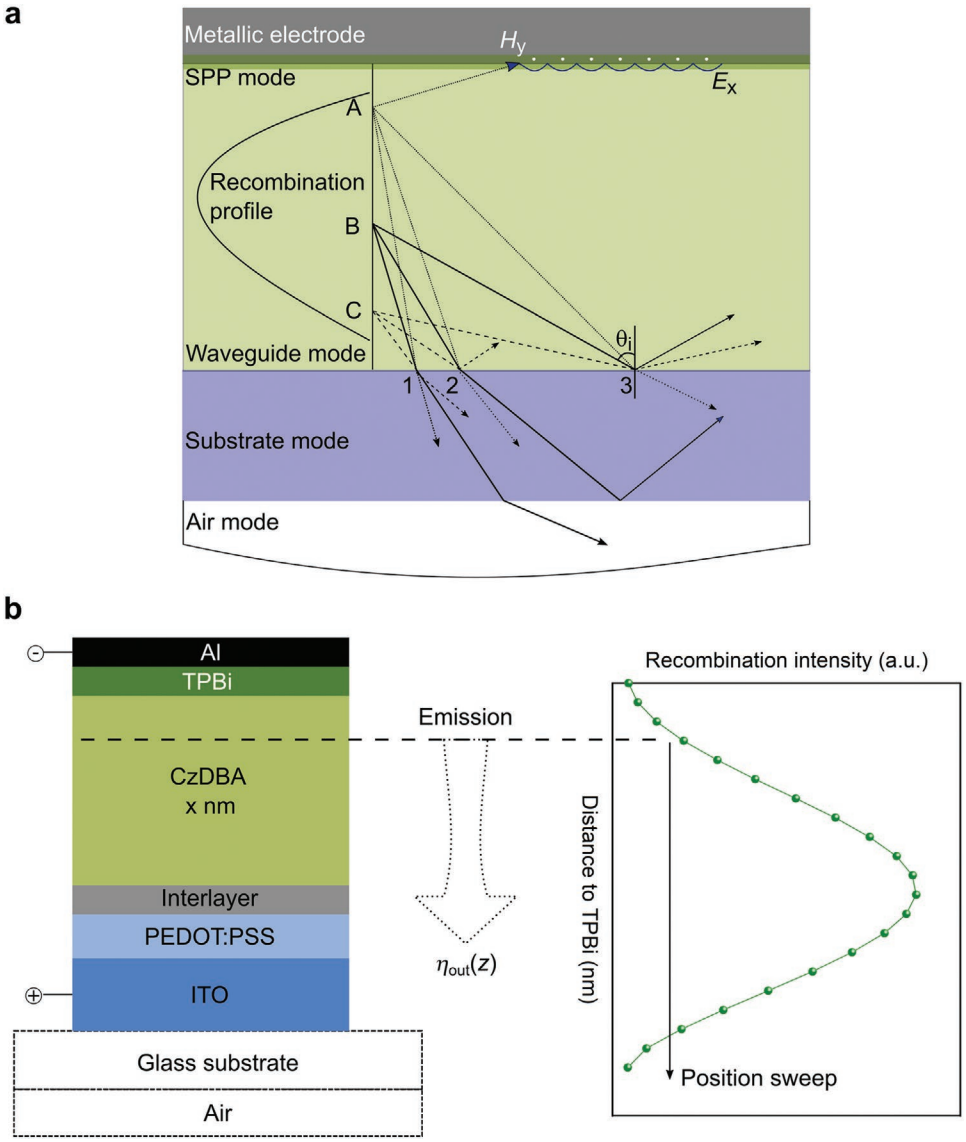

Figure 1. Schematic illustrations of the light outcoupling for OLEDs with a broad recombination zone, based on the CzDBA model system. a) Position-dependent light outcoupling: the incident angle θ_i to the adjacent boundary depends on the emission position within the recombination zone, which is spatially distributed. For example, the incident angle θ_i at position 3 varies depending on the emission position at A (dotted arrows), B (solid arrows), and C (dashed arrows). Light emitted near the metal electrode has a high probability to be captured in the SPP mode at the metal-organic interface. b) Schematic illustration of the CzDBA OLED, where the emission profile is determined by the electrically simulated recombination profile within the thick CzDBA emitting layer.

mode for OLEDs with a strongly confined emission zone can be calculated according to the method developed by Furno et al., in which the anisotropy factor of optical emissive dipole orientation, the layer thickness and optical constants of involved materials are considered.[23] This model has been applied to numerically simulate the outcoupling efficiency for OLEDs, based on the assumption of approximating the emissive plane with a delta-function.[12,24,26–28]

Here, we utilize the single-layer OLEDs based on CzDBA as a model system to simulate the fraction of light emitted into air η_A and the fraction emitted into both substrate and air η_{SA} for devices with a broad recombination zone. CzDBA molecules in the neat film are mostly horizontally oriented, resulting in an anisotropy factor of 0.148 (Figure S1, Supporting Information), which is slightly lower compared to CzDBA doped in host materials.[15] The optical constants for a CzDBA neat film are shown in Figure S2, Supporting Information. Using Equation (5), we first simulate the outcoupling efficiency for different emission positions within the thick emissive layer, where for each position the emission profile is taken as a delta function. Without considering the recombination profile yet, both η_A and η_{SA} are dependent on the emissive position, as well as the cavity thickness, as shown in **Figure 2**a and 2b. An increase of the CzDBA thickness from 50 to 85 nm will raise the maximum light outcoupling into air η_A (Figure 2a) from 19.4% to 28.0%. However, further increase of the layer thickness will reduce the

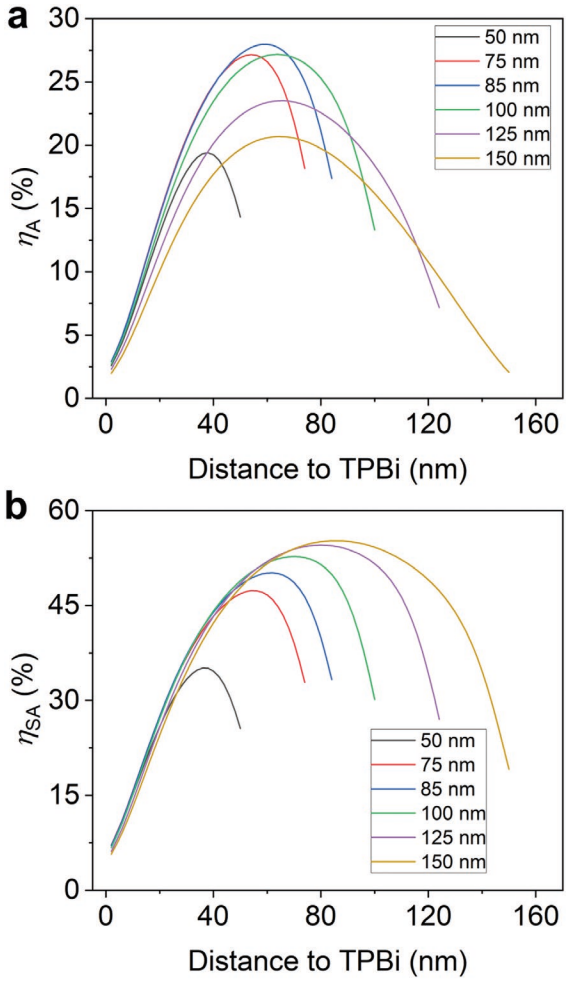

Figure 2. Dependence of the outcoupling efficiency on the CzDBA layer thickness. a) Outcoupling efficiency to the air mode η_A and b) the sum of the substrate and air modes η_{SA} for different positions of the emitting plane (delta function) inside CzDBA layers of varying thickness.

maximum η_A. In the entire range from 50 to 150 nm, the maximum fraction of light coupled into both the substrate and air η_{SA} increases from 35.1% to 55.2%, as presented in Figure 2b. The indium-tin oxide (ITO) thickness has a subtle influence on the optical outcoupling efficiency, with an optimal thickness in the range of 80–120 nm, as shown in Figure S3, Supporting Information.

2.3. Thickness-Dependent Outcoupling Efficiency for OLEDs with a Broad Recombination Profile

Having simulated the position-dependent outcoupling efficiency, we now turn to calculating the outcoupling efficiency for an OLED with a broad recombination profile. As schematically illustrated in **Figure 3**a, for devices with a thick emissive layer, recombination events occur within the entire layer. The recombination profile for OLEDs with different layer thicknesses of CzDBA can be simulated using a numerical drift-diffusion solver.[10] The model includes the electrical energy gap, charge–carrier mobilities, trap densities and energy levels of trap states as well as bimolecular and trap-assisted recombination. The charge–carrier mobility and trap densities for the emitter CzDBA were obtained previously by experiments on single-carrier devices.[10,29] The numerical simulation details can be found in the Experimental Section and Note S1, Supporting Information. The recombination profiles for devices with different CzDBA layer thicknesses at 2.4 V are shown in Figure 2b. The recombination profile naturally broadens with increasing CzDBA layer thickness, with the maximum concomitantly shifting away from the cathode. In general, the peak of the recombination profile is close to the center of CzDBA layer, due to the balanced electron and hole transport.[10]

According to Equation (5), the outcoupling efficiency for devices at 2.4 V can be calculated by weighting η_A and η_{SA} in Figure 2a and 2b with the recombination profile (i.e., Figure 3b). The maximum thickness-dependent η_A and η_{SA} for OLEDs are presented in Figure 3c. It is observed that η_A can be more than 26% for OLEDs with 85 nm CzDBA. Importantly, the outcoupling efficiency is only marginally reduced compared to an OLED with an optimized emitting plane in an optimized cavity, as shown in Figure 2a. This demonstrates that single-layer OLEDs can rival multilayer OLEDs in terms of optical outcoupling. For layer thicknesses below or above the range of 85–100 nm, a decrease in η_A is observed. Meanwhile, η_{SA} reaches ≈52% at 2.4 V when raising the thickness from 50 to 150 nm, showing the potential light outcoupling efficiency when extracting the substrate modes.

Experimentally, the maximum η_{EQE} for single-layer CzDBA OLEDs follows a similar trend when varying the CzDBA layer thickness. The similarity in thickness dependence confirms the derived model. Furthermore, it is observed that the experimental external quantum efficiency is lower than the optical-outcoupling efficiency. According to Equation (4), the absolute difference results from the non-unity internal quantum efficiency, which will be discussed in detail in the following sections.

2.4. Voltage-Dependent Outcoupling Efficiency for OLEDs with a Broad Recombination Profile

Because of the slight difference in charge mobility and trap densities for electrons and holes, the recombination profile is voltage dependent. As shown in Figure 3d, for the device with a CzDBA layer thickness of 85 nm, the recombination profile is shifting towards the ITO side while increasing the driving voltage. A similar shift of the recombination profile for increasing voltage is observed for devices with different CzDBA layer thickness, as presented in Figure S4, Supporting Information. In such case, it is expected that the optical trapping from the SPP mode is reduced.[22] However, according to Equation (5), the highest outcoupling efficiency can only be obtained when the peak of the recombination profile is also close to the optical maximum. Combining the position-dependent outcoupling efficiency shown in Figure 2 with the voltage dependent recombination profile, the η_A and η_{SA} can be calculated as a function of voltage, as presented in Figure 3e and Figure S5, Supporting Information. For devices with an 85 nm CzDBA layer, η_A increases from 24.6% to 26.2% when the voltage is increased

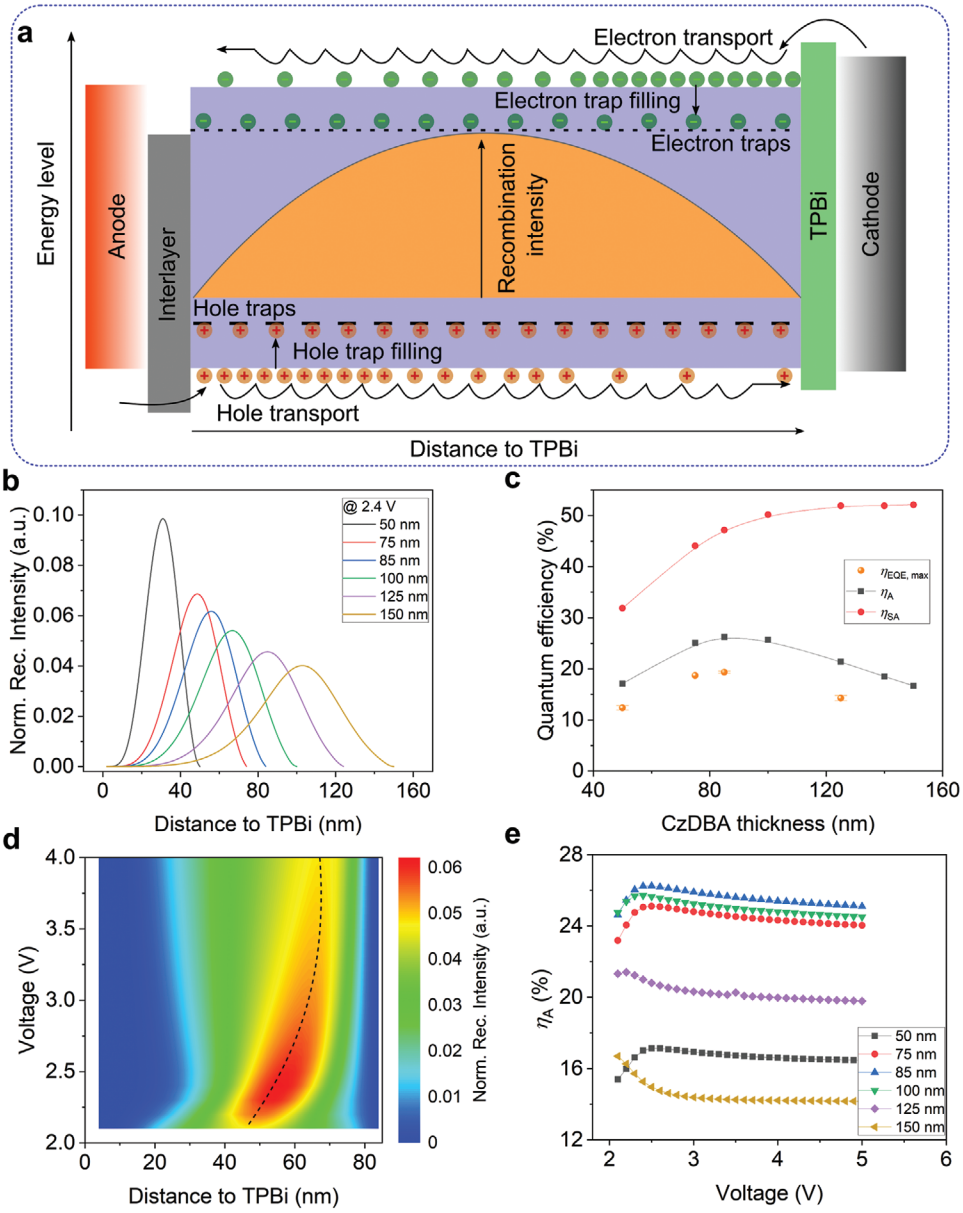

Figure 3. Voltage-dependent outcoupling efficiency for OLEDs with a broad recombination zone. a) Schematic illustration for a voltage and thickness dependent recombination profile. b) Simulated recombination profiles for devices at 2.4 V for different CzDBA layer thickness. c) Comparison of recombination-weighted η_A and η_{SA} for devices at 2.4 V for different CzDBA layer thickness. The experimental maximum η_{EQE} obtained at ≈2.4 V is shown. The error bar is calculated according to the statistics based on different devices. d) Recombination profile normalized to the sum with a step of 2 nm at different driving voltages for devices with 85 nm CzDBA. The dashed line is a guide to the eye for the position of maximum recombination intensity as a function of driving voltage. e) The voltage-dependent outcoupling efficiency η_A for OLEDs with different CzDBA thickness considering the recombination profile.

from 2.1 to 2.5 V, which is a relative increase of 6.5%. By further increasing the driving voltage to 4.0 V, η_A slightly decreases to 25.4%, a relative change of only 3.1%. In this case, the change in η_A contributes more to efficiency roll-on as compared to roll-off, both effects being minor, however. We note that for an 85 nm single-layer CzDBA device, a luminance of 1000 cd m^{-2} is already reached at 2.45 V, demonstrating that high outcoupling efficiency is obtained at practical luminance.

The minor voltage-induced fluctuations in η_A also vary with the thickness of the CzDBA layer. As shown in Figure 3e, for thinner devices, the rise in η_A at low voltage is slightly stronger, while it remains almost constant at higher voltages. For thicker CzDBA layers, the roll-on in outcoupling efficiency is reduced, while the roll-off increases. It should be noted that in all cases the effect of the driving voltage dependence on the outcoupling efficiency is relatively minor in this CzDBA model system.

The voltage dependent η_{SA} can also be simulated in a similar manner. The results for CzDBA devices are summarized in Figure S5, Supporting Information. The maximum η_{SA} increases with increasing layer thickness and can reach ≈50%

for a CzDBA thickness of 125–150 nm. It should be noted that for multi-layer OLEDs with a thicker emission layer, the analysis of the outcoupling efficiency for a broadened emission zone is far more complex, as it requires many input parameters as mobility and trapping in various transport and blocking layers, guest-to-guest transport in the emissive layer and effect of band-offsets on the transport, which all affect the recombination profile. For the single-layer OLED as presented here, a quantitative analysis is straightforward.

According to Equation (5), the outcoupling efficiency η_A for OLEDs with a broad recombination zone should be smaller compared to the case when the emission originates from the optimized position with an ultrathin emissive interface. However, in the case of CzDBA devices here, the final outcoupling efficiency η_A (26.2%) is among the best for many of state-of-the-art OLEDs based on phosphorescent emitters,[22,30] and comparatively close to the maximum in η_A of 28.0% observed for a delta-function emission zone, as shown in Figure 2a.

2.5. Electrical Efficiency for OLEDs with a Broad Recombination Zone

The numerical analysis above has shown that the maximum light-outcoupling efficiency for a CzDBA single-layer OLED amounts to ≈26%. Based on the simulated outcoupling efficiencies and experimentally obtained η_{EQE}, it is possible to further quantify the electrical efficiency of the single-layer OLEDs. Theoretically, the electrical efficiency γ for OLEDs is defined by the ratio between exciton-generation rate and the injected current density J:

$$\gamma = e\frac{\hat{n}_e}{J} = \frac{e\xi\hat{A}}{J} \tag{6}$$

When η_{EQE} for the device is known, it is possible to estimate γ for OLEDs via:

$$\gamma = \frac{\eta_{EQE}}{\eta^*_{int}\cdot\eta_A} \tag{7}$$

For devices based on phosphorescent emitters without strong cavity effect, the photoluminescence quantum yield (PLQY) of the emitter can be treated as η^*_{int}.[23] For TADF emitters, the η^*_{int} is determined by the capability of harvesting the generated triplets as:[12]

$$\eta^*_{int} = \phi_{PF}\left(\frac{0.25}{1-\phi_{ISC}\phi_{rISC}} + \frac{0.75}{1-\phi_{ISC}\phi_{rISC}}\phi_{rISC}\right) \tag{8}$$

where ϕ_{ISC} is the quantum yield of the intersystem crossing for the TADF emitter, ϕ_{rISC} the quantum yield of the reverse intersystem crossing, and ϕ_{PF} the quantum yield of the prompt fluorescence under photon excitation. For the TADF emitter CzDBA, the ratio of quantum yield between the delayed and prompt fluorescence is ≈5, indicating that all the generated triplets under electrical excitation can be transferred to singlets. In such a case, the photoluminescence quantum yield (PLQY) of the CzDBA neat film can be reasonably treated as the η^*_{int} for the single-layer device.[31]

The performance for devices with different CzDBA layer thickness is summarized in **Figure 4**. The difference of current density and voltage dependence behavior can result from the difference of trap numbers and CzDBA layer thickness. For all these devices with different layer thickness, the turn-on voltage determined at 1 cd m^{-2} is close to 2.1 V. As shown in Figure 4b, the maximum η_{EQE} can reach ≈19% for devices with 75–85 nm CzDBA. The external quantum efficiency η_{EQE} is reduced to ≈12% and 14% for devices with 50 and 140 nm CzDBA, respectively. From Figure 4c, it is noted that the maximum luminous efficacy can reach ≈90 lm W^{-1} at a luminance of ≈200 cd m^{-2} for 75 and 85 nm devices. It slightly rolls off to 82 lm W^{-1} at 1000 cd m^{-2}. For all these devices, very similar electroluminescence (EL) spectrum is observed, with the maximum located at a wavelength of 560 nm. A minor change in the EL spectra and also the Commission Internationale de L'Eclairage (CIE) coordinates can be observed for devices with different CzDBA thickness, as shown in Figure 4d and Table S1, Supporting Information, which might result from the different optical cavity length. Furthermore, there is a minor but gradual change of EL spectra when increasing the applied voltages, experimentally demonstrating that the recombination profile is shifting with voltage in devices with a wide recombination zone, which is predicted by the numerical simulations in Figure 3d and Figure S4, Supporting Information.

The experimental η_{EQE}, the simulated η_A, and the calculated electrical efficiency γ for OLEDs of different CzDBA thickness are shown in Figure S7, Supporting Information, according to Equations (6)–(8). The electrical efficiency γ of all devices is shown in **Figure 5**. It is observed that γ is highly dependent on the driving voltage. However, it should be noted that for single-layer CzDBA OLEDs, a broad variation in brightness is observed in a very narrow voltage window, resulting in high electrical efficiencies over a large range in luminance. For devices with an 85 nm CzDBA layer, γ increases from 50.0% at 2.1 V (turn-on voltage) to 83.2% at 2.3 V (200 cd m^{-2}), and drops to 47.1% at 4 V (20 000 cd m^{-2}). The maximum electrical efficiency γ reaches values of up to 92%, as observed for the device with a 140 nm CzDBA layer. A detailed analysis for each layer thickness is shown in Figure S7, Supporting Information. For all devices, both γ and η_A have very pronounced variation at low driving voltages. We now further explore the mechanism of efficiency roll-on for the device shown here.

According to Equation (6), the electrical efficiency γ is directly related to the generated exciton density. Non-radiative recombination events or annihilation processes between excitons or excitons and polarons can lead to the decrease of electrical efficiency γ from unity. Bimolecular processes can play an important role in the efficiency roll-off at high voltages when the exciton concentration is high.[32,33] However, at low voltages, the increase in electrical performance should have a different origin.

According to our previous study, in the single-layer CzDBA device there are hole traps with a density of 1.7×10^{16} cm^{-3} and electron traps with a density of 1.4×10^{16} cm^{-3}, respectively.[10] Compared to other emitters such as 1,2,3,5-tetrakis(carbazol-9-yl)-4,6-dicyanobenzene (4CzIPN), poly[2-methoxy-5-(2-ethylhexyloxy)-1,4-phenylenevinylene] (MEH-PPV) or poly(9,9-dioctylfluorene-alt-benzothiadiazole) (F8BT), the trap densities

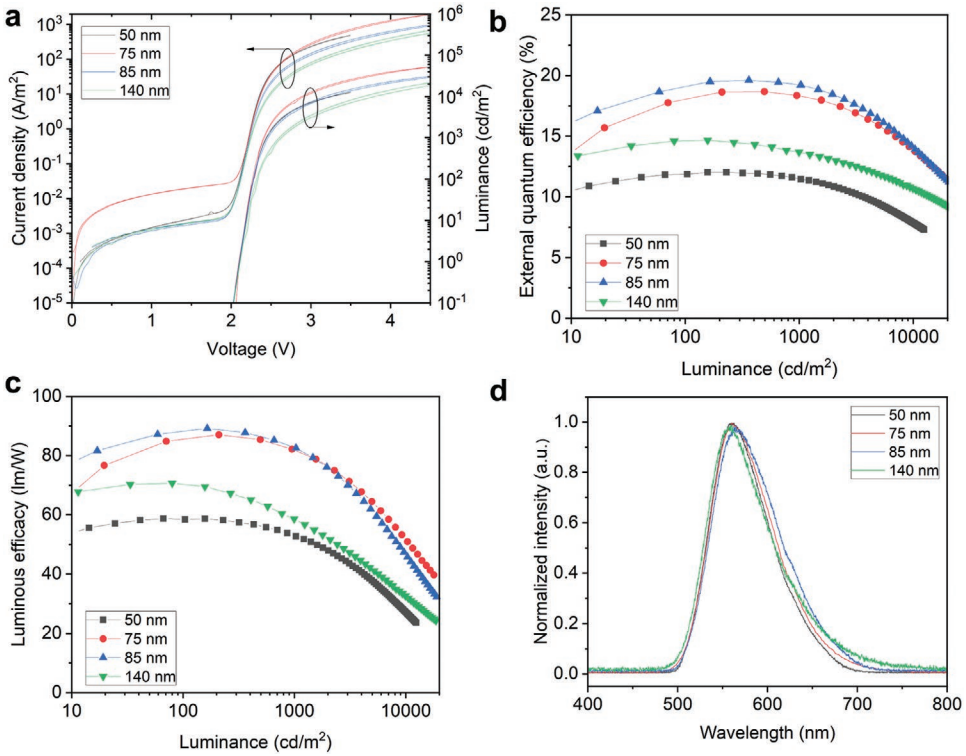

Figure 4. Device performance for OLEDs with different CzDBA layer thickness. a) Current density–voltage–luminance characteristics, b) external quantum efficiency versus luminance, c) luminous efficacy versus luminance, and d) electroluminescence spectra.

for holes and electrons of CzDBA are at least an order of magnitude lower.[14,34,35] Traps in these devices can therefore already be gradually filled at low voltages, as illustrated in Figure 3a. Upon trap filling, the bimolecular Langevin recombination becomes dominant over the non-radiative trap-assisted recombination, giving rise to an increase of electrical efficiency when raising the voltage, and thereby the charge–carrier density in this regime, as shown in Figure 5. The decrease of the electrical efficiency at higher voltage is a subject of further study.

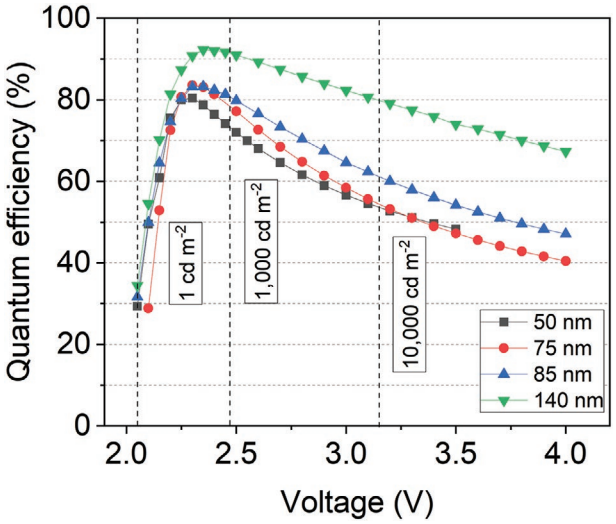

Figure 5. Electrical quantum efficiency for CzDBA single-layer OLEDs. The η_{EQE} is experimentally measured, while η_A is simulated by considering the recombination profile. The dashed lines indicate the voltages at which some typical luminance levels for the device with 85 nm CzDBA are obtained.

3. Conclusion

In this work, we analyzed the effect of a broad recombination zone in OLEDs on the optical outcoupling efficiency. We first presented a methodology to simulate the fraction of light coupled into the air and/or substrate for OLEDs with a spatially distributed recombination zone. It is demonstrated that the outcoupling efficiency can be calculated by numerical integration over different positions of emitting dipoles, weighted by the sum-normalized recombination profile. As a model system, we analyzed the outcoupling efficiency of OLEDs based on a single layer of the TADF emitter CzDBA. Here, the recombination zone distributes over the entire emissive layer, with the profile depending on the layer thickness and driving voltages. A fraction of ≈26% generated photons can escape to air mode for the optimized device, which is comparable to multilayer devices exploiting an ultrathin emission zone in an optimized cavity. Based on the experimental external quantum efficiency and the simulated outcoupling efficiency, it is possible to further obtain the voltage-dependence of the electrical efficiency. The increase in electrical efficiency at low driving voltages can be attributed to trap filling, prior to reaching a maximum internal efficiency of 92%.

Our study demonstrates how to treat optical outcoupling in devices with a broadened recombination profile. Unlike previous investigations of the optical outcoupling of OLEDs,

we here couple the optical model with electrical simulations of the recombination profile, based on experimentally validated charge–transport parameters. It is shown that broadening of the recombination zone does not go at the expense of the optical outcoupling efficiency, while retaining the benefits of a simplified architecture and enhanced operational stability.

4. Experimental Section

OLED Fabrication: ITO(120 nm)-covered glass substrates were thoroughly cleaned with detergent solution, followed with ultrasonic bath in acetone and isopropyl alcohol. Subsequently, the ITO substrates were treated by UV–ozone. A 40 nm layer of poly(3,4-ethylenedioxythiophene):polystyrene sulfonate (PEDOT:PSS) was spin coated and annealed at 140 °C for 10 min in air. The substrates were then transferred into evaporation chambers with a base pressure of 4–6 $\times$ 10^{-7} mbar to deposit the following functional layers. Organic functional materials and inorganic layers were deposited in separate chambers. The evaporation rates and layer thicknesses are tracked by quartz crystal monitors. A 6 nm MoO_3 layer, a 3 nm C_{60} interlayer, a CzDBA emissive layer, and a 4 nm 2,2′,2″-(1,3,5-Benzinetriyl)-tris(1-phenyl-1-H-benzimidazole) (TPBi) layer were sequentially thermally deposited for the experimental OLEDs investigated in this work. A 100 nm aluminum layer was deposited as the cathode. The devices were characterized in a nitrogen-filled glove box without further encapsulation.

Device Characterization: The current density-voltage characterization was carried out with a Keithley 2400 source meter, while the light output was recorded simultaneously with a (NIST traceable) calibrated Si photodiode with an area larger than the emissive pixel, placed in close proximity to the emitting surface in order to capture all light emitted in the forward hemisphere. The substrate edges of the OLEDs were sealed by the sample holder to avoid detection of the waveguided light from the substrate mode. EL spectra were obtained with a USB4000-UV-VIS-ES spectrometer at different driving voltages. The luminance, η_{EQE}, and luminous efficacy was calculated according to a previously published method.[36,37]

Recombination Profile Simulations: The numerical simulation of the recombination profile for the single-layer device was performed using a model described previously, in which the built-in voltage, electrical energy gap for the emitter, trap density for holes and electrons, and charge–carrier mobility are considered.[38] The electrical energy gap for the emitter was calculated as the sum of the optical energy gap and the exciton energy, in which the exciton energy is assumed to be 0.4 eV.[39,40] The charge transport parameters for CzDBA as determined in the work of Liu et al.[29] were used. The bimolecular-recombination profile responsible for the emission was simulated at different driving voltages by assuming a Langevin recombination rate. A more detailed theoretical description can be found in the Note S1, Supporting Information.

Optical Characterization: The outcoupling efficiency simulation at different positions within the recombination zone is based on a previously developed model, as described in detail in the main text, which has been successfully used for OLEDs based on phosphorescent and conventional emitters.[23,24] The optical simulation is based on the harmonic oscillator model of an emissive dipole within a cavity, with an anisotropy factor to describe the orientation of the transition dipole moment. For PEDOT:PSS, MoO_3, C_{60}, TPBi, and Al, complex refractive indices are considered. The refractive index of CzDBA was experimentally determined by a variable angle spectroscopic ellipsometer (Alpha-SE, Quantum Design GmbH). The dipole orientation of the CzDBA neat film was determined with a Fluxim Phelos gonio-spectrometer by fitting the angular dependence of photoluminescence with Setfos software from Fluxim.

Supporting Information

Supporting Information is available from the Wiley Online Library or from the author.

Acknowledgements

The authors thank Dr. Mauro Furno for developing the simulation script for OLEDs with a delta-function distributed recombination profile and Prof. Dr. Karl Leo at TU Dresden for the application permission.

Open access funding enabled and organized by Projekt DEAL.

Conflict of Interest

The authors declare no conflict of interest.

Data Availability Statement

Research data are not shared.

Keywords

device lifetime, organic light-emitting diodes, outcoupling efficiency, recombination profile, thermally activated delayed fluorescence

Received: October 20, 2020
Revised: February 8, 2021
Published online:

[1] C. W. Tang, S. A. VanSlyke, *Appl. Phys. Lett.* **1987**, *51*, 913.
[2] K. Walzer, B. Maennig, M. Pfeiffer, K. Leo, *Chem. Rev.* **2007**, *107*, 1233.
[3] M. Thompson, *MRS Bull.* **2007**, *32*, 694.
[4] A. Salehi, X. Fu, D.-H. Shin, F. So, *Adv. Funct. Mater.* **2019**, 1808803.
[5] H. Uoyama, K. Goushi, K. Shizu, H. Nomura, C. Adachi, *Nature* **2012**, *492*, 234.
[6] M. Y. Wong, E. Zysman-Colman, *Adv. Mater.* **2017**, *29*, 1605444.
[7] S. K. Jeon, H. L. Lee, K. S. Yook, J. Y. Lee, *Adv. Mater.* **2019**, *31*, 1803524.
[8] L.-S. Cui, S.-B. Ruan, F. Bencheikh, R. Nagata, L. Zhang, K. Inada, H. Nakanotani, L.-S. Liao, C. Adachi, *Nat. Commun.* **2017**, *8*, 2250.
[9] D. Zhang, M. Cai, Y. Zhang, D. Zhang, L. Duan, *Mater. Horiz.* **2016**, *3*, 145.
[10] N. B. Kotadiya, P. W. M. Blom, G.-J. A. H. Wetzelaer, *Nat. Photonics* **2019**, *13*, 765.
[11] Y. Li, Z. Tang, C. Hänisch, P.-A. Will, M. Kovačič, J.-L. Hou, R. Scholz, K. Leo, S. Lenk, S. Reineke, *Adv. Opt. Mater.* **2019**, *7*, 1801262.
[12] Y. Li, Q. Wei, L. Cao, F. Fries, M. Cucchi, Z. Wu, R. Scholz, S. Lenk, B. Voit, Z. Ge, S. Reineke, *Front. Chem.* **2019**, *7*, 688.
[13] N. B. Kotadiya, H. Lu, A. Mondal, Y. Ie, D. Andrienko, P. W. M. Blom, G. J. A. H. Wetzelaer, *Nat. Mater.* **2018**, *17*, 329.
[14] N. B. Kotadiya, A. Mondal, P. W. M. Blom, D. Andrienko, G. J. A. H. Wetzelaer, *Nat. Mater.* **2019**, *18*, 1182.
[15] T.-L. Wu, M.-J. Huang, C.-C. Lin, P.-Y. Huang, T.-Y. Chou, R.-W. Chen-Cheng, H.-W. Lin, R.-S. Liu, C.-H. Cheng, *Nat. Photonics* **2018**, *12*, 235.
[16] S. Reineke, M. Thomschke, B. Luessem, K. Leo, *Rev. Mod. Phys.* **2013**, *85*, 1245.
[17] Z. Wu, D. Ma, *Mater. Sci. Eng., R* **2016**, *107*, 1.
[18] Q. Niu, R. Rohloff, G.-J. A. H. Wetzelaer, P. W. M. Blom, N. I. Crăciun, *Nat. Mater.* **2018**, *17*, 557.
[19] S. Kim, H. J. Bae, S. Park, W. Kim, J. Kim, J. S. Kim, Y. Jung, S. Sul, S.-G. Ihn, C. Noh, S. Kim, Y. You, *Nat. Commun.* **2018**, *9*, 1211.

[20] J. Lee, C. Jeong, T. Batagoda, C. Coburn, M. E. Thompson, S. R. Forrest, *Nat. Commun.* **2017**, *8*, 15566.
[21] S. Hofmann, M. Thomschke, P. Freitag, M. Furno, B. Lüssem, K. Leo, *Appl. Phys. Lett.* **2010**, *97*, 253308.
[22] R. Meerheim, M. Furno, S. Hofmann, B. Lüssem, K. Leo, *Appl. Phys. Lett.* **2010**, *97*, 253305.
[23] M. Furno, R. Meerheim, S. Hofmann, B. Lüssem, K. Leo, *Phys. Rev. B* **2012**, *85*, 115205.
[24] Y. Li, M. Kovačič, J. Westphalen, S. Oswald, Z. Ma, C. Hänisch, P. Will, L. Jiang, M. Junghaehnel, R. Scholz, S. Lenk, S. Reineke, *Nat. Commun.* **2019**, *10*, 2972.
[25] S. Hofmann, M. Thomschke, B. Lüssem, K. Leo, *Opt. Express* **2011**, *19*, A1250.
[26] J. Ràfols-Ribé, P.-A. Will, C. Hänisch, M. Gonzalez-Silveira, S. Lenk, J. Rodríguez-Viejo, S. Reineke, *Sci. Adv.* **2018**, *4*, eaar8332.
[27] J. Song, K. H. Kim, E. Kim, C. K. Moon, Y. H. Kim, J. J. Kim, S. Yoo, *Nat. Commun.* **2018**, *9*, 3207.
[28] J. Lee, T.-H. Han, M.-H. Park, D. Y. Jung, J. Seo, H.-K. Seo, H. Cho, E. Kim, J. Chung, S.-Y. Choi, T.-S. Kim, T.-W. Lee, S. Yoo, *Nat. Commun.* **2016**, *7*, 11791.
[29] W. Liu, N. B. Kotadiya, P. W. M. Blom, G. J. A. H. Wetzelaer, D. Andrienko, *Adv. Mater. Technol.* **2020**, *6*, 2000120.
[30] M. Furno, T. C. Rosenow, M. C. Gather, B. Lüssem, K. Leo, *Appl. Phys. Lett.* **2012**, *101*, 143304.
[31] F. B. Dias, T. J. Penfold, A. P. Monkman, *Methods Appl. Fluoresc.* **2017**, *5*, 012001.
[32] S. Reineke, G. Schwartz, K. Walzer, K. Leo, *Appl. Phys. Lett.* **2007**, *91*, 123508.
[33] S. Reineke, K. Walzer, K. Leo, *Phys. Rev. B: Condens. Matter Mater. Phys.* **2007**, *75*, 125328.
[34] Y. Zhang, B. de Boer, P. W. M. Blom, *Phys. Rev. B: Condens. Matter Mater. Phys.* **2010**, *81*, 085201.
[35] H. T. Nicolai, M. Kuik, G. A. H. Wetzelaer, B. de Boer, C. Campbell, C. Risko, J. L. Brédas, P. W. M. Blom, *Nat. Mater.* **2012**, *11*, 882.
[36] S. R. Forrest, D. D. C. Bradley, M. E. Thompson, *Adv. Mater.* **2003**, *15*, 1043.
[37] M. Anaya, B. P. Rand, R. J. Holmes, D. Credgington, H. J. Bolink, R. H. Friend, J. Wang, N. C. Greenham, S. D. Stranks, *Nat. Photonics* **2019**, *13*, 818.
[38] M. Kuik, G. J. A. H. Wetzelaer, H. T. Nicolai, N. I. Craciun, D. M. De Leeuw, P. W. M. Blom, *Adv. Mater.* **2014**, *26*, 512.
[39] J. L. Bredas, *Mater. Horiz.* **2014**, *1*, 17.
[40] V. Coropceanu, J. Cornil, D. Silva, D. A, Y. Olivier, R. Silbey, J. L. Bredas, D. A. da Silva Filho, J.-L. J.-L. Brédas, Y. Olivier, R. Silbey, J.-L. J.-L. Brédas, *Chem. Rev.* **2007**, *107*, 926.